ENHANCED TRANSDUCTION METHODS FOR ELECTROSTATICALLY DRIVEN MEMS RESONATORS

A. T-H. Lin, J. E-Y. Lee, J. Yan, A. A. Seshia
Department of Engineering, Trumpington Street, University of Cambridge,
Cambridge, UNITED KINGDOM

ABSTRACT

Electrically addressed silicon bulk acoustic wave microresonators offer high Q solutions for applications in sensing and signal processing. However, the electrically transduced motional signal is often swamped by parasitic feedthrough in hybrid technologies. With the aim of enhancing the ratio of the motional to feedthrough current at nominal operating voltages, this paper benchmarks a variety of drive and detection principles for electrostatically driven square-extensional mode resonators operating in air and in a foundry MEMS process utilizing 2μm gaps. A new detection technique, combining second harmonic capacitive actuation and piezoresistive detection, outperforms previously reported methods utilizing voltages as low as ± 3V in air providing a promising solution for low voltage CMOS-MEMS integration.

KEYWORDS

BAW resonator, harmonic driving, piezoresistive sensing

INTRODUCTION

Silicon bulk acoustic wave (BAW) resonators offer high Q solutions to a variety of applications such as timing references, filters and precision sensors. However, due to the relatively high stiffnesses and large motional resistance, the motional signal is often swamped by parasitic feedthrough in hybrid technologies. Although integration with CMOS results in lower capacitive parasitics, the resonator bias voltages are often limited to less than 5V. Reducing the transduction gap decreases the motional resistance but limits motional amplitude. The realization of sub-micron transduction gaps relies on advanced fabrication technology that often requires careful control on the definition of sidewall spacers and/or sacrificial layers. The latter often places significant constraints on the MEMS fabrication process, integration with CMOS and ultimately device yield.

Various studies have been devoted on actuation and detection principles with the aim to enhance the motional to feedthrough current ratio [1-4]. This paper benchmarks these principles for an electrostatically driven square-extensional mode resonator operating in air and fabricated in a foundry MEMS process utilizing 2μm gaps. The aim is to illustrate techniques and principles that enhance the ratio of the motional to feedthrough current at nominal operating voltages. A new detection technique is also introduced by combining second harmonic capacitive actuation and piezoresistive detection. This method outperforms previously reported methods utilizing voltages as low as ± 3V in air.

DEVICE DESCRIPTION

The tested device is a 2.2MHz square plate resonator operated in the bulk extensional mode, with parameters as shown in Table 1. The resonator is fabricated in a commercial SOI foundry process (MEMSCAP), with one electrode on each side of the square plate. An electrical connection is provided to each anchor of the resonator body. This enables the capacitive and piezoresistive sensing configurations used in this work. An optical micrograph of the resonator is shown in Fig. 1.

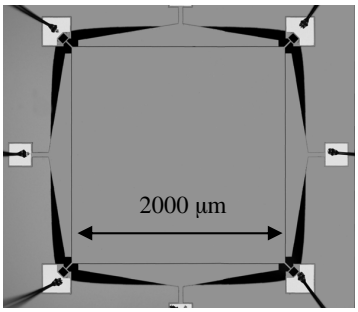

Figure 1: Optical micrograph of the square resonator fabricated by the MEMSCAP SOIMUMPs process.

Table 1: Resonator parameters

Parameters	Symbol	Value
Side length	*L*	2000 μm
Thickness	*H*	25 μm
Transduction gap	*g*	2 μm
Resonant frequency	*f*	2.2 MHz
Measured quality factor	*Q*	6771

MEASUREMENT THEORY & SETUP

This section presents the theory behind the progression of electrostatic methods for reducing feedthrough and introduces piezoresistive sensing methods for increasing motional signal. This model sets up the six transduction methods that are documented and compared, as summarized in table 2.

Electrostatic actuation and sensing

For a parallel plate electrostatic actuator, the actuation force is given by

$$F = \frac{1}{2}\left(\frac{\partial C}{\partial x}\right)V^2 \quad (1)$$

where V is the applied voltage, x is the resonator displacement, $C = \frac{\varepsilon_0 A}{g}$ is the capacitance of the parallel plate, and ε_0, g, A are the permittivity, transduction gap and transduction area respectively. For a one-port configuration as shown in figure 2a, using fundamental frequency driving, the input voltage can be written as the sum of a DC bias V_{dc} and an AC signal $V_{ac} = |V_{ac}|\cos\omega_0 t$ at resonant frequency ω_0, yielding the expression for actuator force

$$F = V_{dc}|V_{ac}|\cos\omega_0 t\frac{\partial C}{\partial x} = F_0\cos\omega_0 t$$

where $F_0 = V_{dc}|V_{ac}|\frac{\partial C}{\partial x}$ (2)

Although maximizing electrode area maximizes the capacitive motional current in a one port configuration, the feedthrough current can also be substantially large as the actuator capacitor also serves to capacitively couple the resonator body to the surrounding electrodes.

By using separate electrodes for driving and sensing, as shown in figure 2b, the two port configuration can reduce feedthrough through the direct overlap capacitor between the actuator electrodes and the resonator [2]. However, feedthrough between drive and sense electrodes could still exist through the substrate or the package, which can mask the motional current.

Shifting the feedthrough current relative to the motional current in the frequency domain utilizes the high-Q resonant response to filter the feedthrough current at the resonant frequency [1, 2]. The nonlinearity of electrostatic transduction can be utilized to drive the structure with a harmonic voltage at half the resonant frequency:

$$V_{ac} = |V_{ac}|\cos\frac{\omega_0}{2}t$$

This results in a force at the resonant frequency, given by

$$F = \frac{|V_{ac}|^2}{4}\cos\omega_0 t\frac{\partial C}{\partial x} = F_0\cos\omega_0 t$$

where $F_0 = \frac{|V_{ac}|^2}{4}\frac{\partial C}{\partial x}$ (3)

However, the feedthrough effect from the harmonics of the driving signal, albeit much smaller, can still be observed.

If two AC input frequencies are available, the device can be driven by off resonance signals V_{RF} and V_{LO}. From equation 1, this generates a force at their sum or difference frequency. By setting the input frequencies ω_{RF}, ω_{LO} such that $\omega_0 = \omega_{RF} + \omega_{LO}$, The actuation force is given by

$$F = \frac{1}{2}|V_{RF}||V_{LO}|\cos\omega_0 t\frac{\partial C}{\partial x} = F_0\cos\omega_0 t$$

where $F_0 = \frac{1}{2}|V_{RF}||V_{LO}|\frac{\partial C}{\partial x}$ (4)

This mixing setup is shown in figure 2c. In this approach, if the harmonics of the driving signal do not overlap with the sensing signal, the feedthrough effect is minimized. However, with capacitive sensing, a DC bias is required, as the motional current is given by

$$i_m = V_{dc}\left(\frac{\partial C}{\partial x}\right)\dot{x} \quad (5)$$

The maximum displacement at resonance for a given actuation force can be expressed as

$$X_0 = \frac{F_0 Q}{m_{eq}\omega_0^2} \quad (6)$$

where Q, m_{eq} are the quality factor and equivalent mass of the resonator. Substituting the force equations (2-4) and displacement equation (6) into (5), the motional current for each capacitive measurement method was derived, as summarized in table 2. It can be seen that the capacitive sensing signal is limited by the transduction gap, as the motional current is proportional to V_{dc} and inversely proportional to g^4.

Piezoresistive sensing

Apart from capacitive measurement techniques, the mechanical motion of the square plate operating in the bulk extensional mode can also be detected through the variation in the electrical resistance of the vibrating structure due to the piezoresistive effect of single crystal silicon. This method has been previously shown to be a promising alternative for increasing the amplitude of the motional signal [3, 4]. In this work, the electrical resistance between two corners of the square plate is monitored by applying a voltage difference, as shown in figure 2d. The motional current measured is proportional to the change in resistance $\frac{\Delta R}{R}$ of the resonator structure and the applied DC voltage V_d, given by

$$I_m \approx \frac{V_d}{R}\left(\frac{\Delta R}{R}\right) \quad (7)$$

where $R = R_r + R_s$, and R_r, R_s are the resistance of the resonator and the resistance of the externally controlled resistor respectively. The change in resistance due to piezoresistivity follows

$$\frac{\Delta R}{R_r} = \pi_t\sigma_t + \pi_l\sigma_l \quad (8)$$

where π_l, π_t are the longitudinal and transverse pezoresistive coefficients, and σ_l, σ_t are the longitudinal and transverse stresses respectively. An approximate

analytical model can be developed to relate the stresses in the resonator for the extensional mode to the change in resistance between the two diagonal corners of the square plate:

$$\frac{\Delta R}{R_r} = \frac{0.8 E_{SE} X_0}{L}(\pi_t + \pi_l) \qquad (9)$$

where L, H, E_{SE} are the length, thickness and bi-axial modulus of the square plate.

The motional signal can be enhanced independent of the driving signal and the transduction gap, and can be significantly larger than capacitive measurements. The current through the resonator can be tuned by setting V_d, and is ultimately limited by the maximum current density ceiling for single crystal silicon and the electrical power dissipated in the resonator. All four electrodes can be utilized for electrostatic actuation of the square extensional mode.

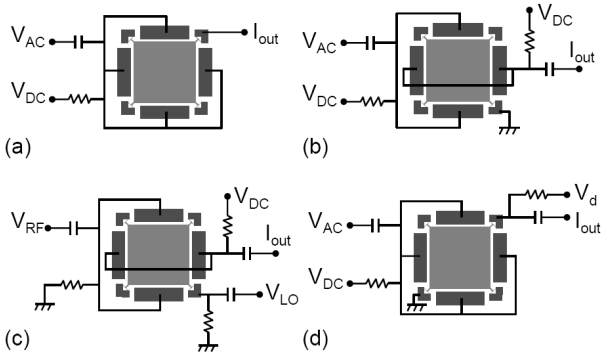

Figure 2: Schematic showing measurement setups for (a) One port, (b) Two port, (c) Mixing and (d) Piezoresistive sensing.

RESULTS & DISCUSSION

Figure 3 shows the measurements results for each transduction scheme employed for the same square extensional mode resonator. All the measurements are done at atmospheric pressure. For capacitive sensing of the motional current, a DC bias of 30V was applied between the resonator and the electrode.

One port and two port measurements

A comparison between one port and two port measurements for fundamental frequency capacitive drive and sensing demonstrate a small signal enhancement utilizing the two port scheme as compared to the one port measurement, as shown in Figs. 3a and 3b.

Harmonic driving and mixing measurements

Measurements for 2nd harmonic and mixing techniques successfully allows feedthrough currents to be rejected by separating them from the motional current in the frequency domain and showed enhanced signal amplitudes of 8 dB (Fig. 3c) and 9 dB (Fig. 3d) respectively. The difference is due to the fact that 2nd harmonic driving is limited by feedthrough from the harmonics of the drive signal, whereas the drive signal for the mixing method can be selected to reject harmonics overlapping with the detection frequency.

Piezoresistive sensing measurements

The one port capacitive driving and piezoresistive sensing measurements showed a peak height of 0.5dB with 5mA drain current, as shown in figure 3e. This is an improvement to the one/two-port capacitive sensing scheme. Note that in this configuration, the detected signal contains both the capacitive and piezoresistive components of the motional current.

Further signal enhancement is achieved by combining second harmonic drive and piezoresistive sensing. This allows the rejection of feedthrough currents as well as eliminates the need of a large DC bias for driving and sensing. Figure 3f demonstrates the measured signal with peak height of 13dB, an AC actuation voltage of ± 3V, a DC Voltage of -2V and drain current of 5mA.

Comparing all the measurement results, we can see that the distortion of the measured resonant peak due to parasitic feedthrough is visible in the one/two-port measurement, and is substantially rejected in the harmonic driving and mixing measurements, and almost unnoticeable in the piezoresistive sensing measurements. The extracted quality factor for the two-port measurement is 6771.

Thus, piezoresistive sensing combined with second harmonic drive is a viable transduction principle for electrically interrogated BAW resonators with micron-scale gaps and limited supply voltage. As compared to [3], there is no modification to the structural design of the resonator and a large transduction area is available for actuation. We are extending this principle to combine the capacitive mixing drive with piezoresistive sensing to obtain further signal enhancement.

CONCLUSIONS

Six transduction methods were documented and compared for electrically characterizing a square extensional mode resonator. We have demonstrated that piezoresistive sensing combined with second harmonic drive is a viable transduction principle for electrically interrogated BAW resonators with micron-scale transduction gaps. This method outperforms previously reported methods utilizing voltages as low as ± 3V in air providing a promising solution for low voltage CMOS-MEMS integration.

REFERENCES

[1] V. J. Logeeswaran, F. E. H. Tay, M. L. Chan, F. S. Chau, and Y. C. Liang, "First harmonic (2f) characterisation of resonant frequency and Q-factor of

micromechanical transducers," *Analog Integrated Circuits and Signal Processing*, vol. 37, pp. 17-33, Oct 2003.

[2] J. R. Clark, W. T. Hsu, M. A. Abdelmoneum, and C. T. C. Nguyen, "High-Q UHF micromechanical radial-contour mode disk resonators," *J. Microelectromech. Syst.*, vol. 14, pp. 1298-1310, Dec 2005.

[3] J. T. M. Van Beek, P. G. Steeneken, and B. Giesbers, "A 10MHz piezoresistive MEMS resonator with high Q," *Proceedings of the 2006 IEEE International Frequency Control Symposium and Exposition*, Vols 1 and 2, pp. 475-480, 2006.

[4] D. Weinstein and S. A. Bhave, "Piezoresistive sensing of a dielectrically actuated silicon bar resonator," in *Solid-State Sensors, Actuators, and Microsystems Workshop*, Hilton Head Island, South Carolina, 2008, pp. 368-371.

CONTACT

* A.A. Seshia, tel: +44-1223-760333; aas41@cam.ac.uk

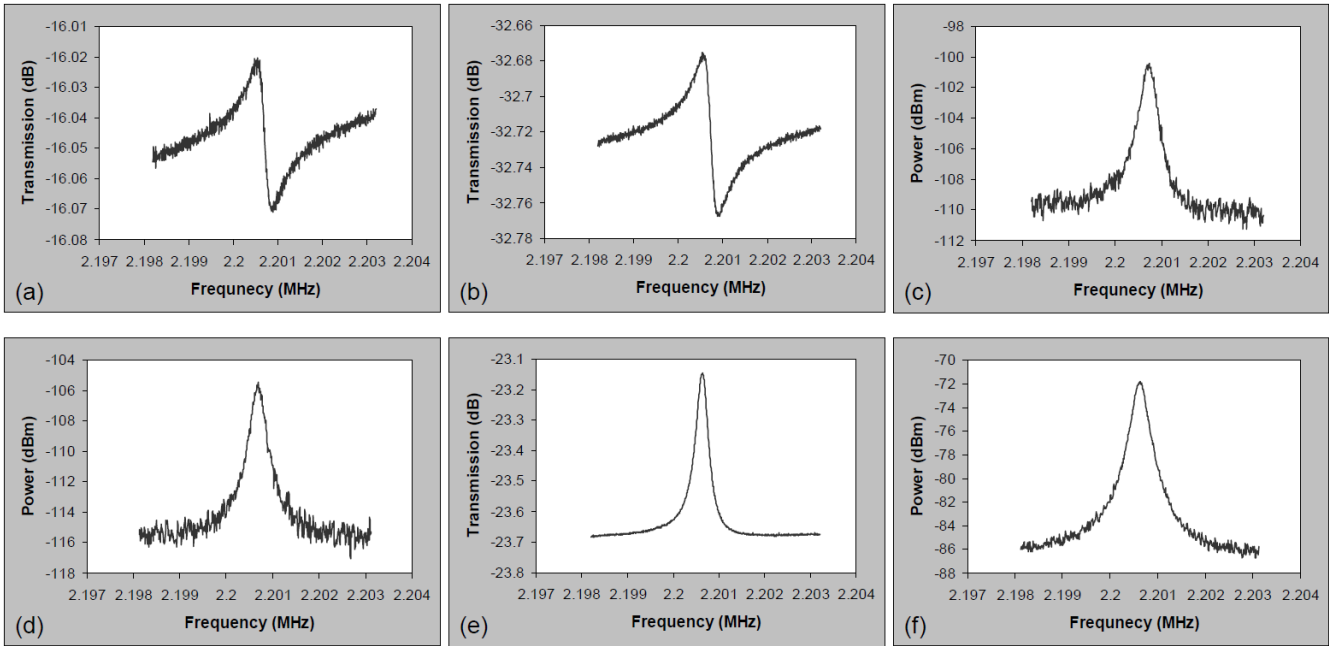

Figure 3: Measured frequency response for a 2.2MHz square extensional mode resonator in air using (a) One port, (b) Two port, (c) Second harmonic, (d) mixing measurements, (e) One port capacitive drive with piezoresistive sensing and (f) second harmonic drive with piezoresistive sensing. The parameters for each measurement are shown in table 2.

Table 2: Summary of transduction methods, where $\omega_0, m_{eq}, Q, \varepsilon_0, A$ are the angular resonant frequency, equivalent mass of the resonator, quality factor, permittivity of air and transduction area respectively.

Transduction methods	Actuation force (F_0)	Motional current ($\lvert I_m \rvert$)	Parameters	Peak height
One port	$V_{dc}\lvert V_{ac}\rvert\frac{\varepsilon_0 A}{g^2}$	$\frac{\lvert V_{dc}\rvert^2\lvert V_{ac}\rvert Q\varepsilon_0^2 A^2}{m_{eq}\omega_0 g^4}$	$V_{dc}=30V$ $V_{ac}=0dBm$	~ 0.02 dB
Two port	$V_{dc}\lvert V_{ac}\rvert\frac{\varepsilon_0 A}{g^2}$	$\frac{\lvert V_{dc}\rvert^2\lvert V_{ac}\rvert Q\varepsilon_0^2 A^2}{m_{eq}\omega_0 g^4}$	$V_{dc}=30V$ $V_{ac}=0dBm$	~ 0.04 dB
2nd harmonic	$\frac{\lvert V_{ac}\rvert^2}{4}\frac{\varepsilon_0 A}{g^2}$	$\frac{\lvert V_{dc}\rvert\lvert V_{ac}^2\rvert Q\varepsilon_0^2 A^2}{4m_{eq}\omega_0 g^4}$	$V_{dc}=30V$ $V_{ac}=\pm 3V$	~ 8 dB
Mixing	$\frac{1}{2}\lvert V_{RF}\rvert\lvert V_{LO}\rvert\frac{\varepsilon_0 A}{g^2}$	$\frac{\lvert V_{dc}\rvert\lvert V_{RF}\rvert\lvert V_{LO}\rvert Q\varepsilon_0^2 A^2}{2m_{eq}\omega_0 g^4}$	$V_{dc}=30V$ $V_{RF}=\pm 3V, V_{LO}=\pm 3V$	~ 9 dB
One port driving & piezoresistive sensing	$V_{dc}\lvert V_{ac}\rvert\frac{\varepsilon_0 A}{g^2}$	$\frac{\Delta R}{R}\left(\frac{V_d}{R}\right)$	$V_{dc}=30V, V_{ac}=0dBm$ $V_d=-2V, I_d=5mA$	~ 0.5 dB
2nd harmonic driving & piezoresistive sensing	$\frac{\lvert V_{ac}\rvert^2}{4}\frac{\varepsilon_0 A}{g^2}$	$\frac{\Delta R}{R}\left(\frac{V_d}{R}\right)$	$V_{ac}=\pm 3V$ $V_d=-2V, I_d=5mA$	~ 13 dB